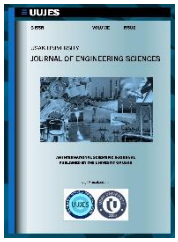

Usak University

Journal of Engineering Sciences

An international e-journal published by the University of Usak

Journal homepage: dergipark.gov.tr/uujes

Research article

COMPARATIVE STUDY ON THE IMPACT OF COLLECTOR GEOMETRY ON ELECTROSPUN NANOFIBER MORPHOLOGY AND POROSITY USING MULTIPLE POLYMERS

Fatma Kuru

Molecular Nano-Materials Laboratory, University of Mugla Sitki Kocman, Turkey

Received: May 7, 2025 *Revised: June 5, 2025* *Accepted: June 17, 2025*
Online available: June 30, 2025

Abstract

In this study, nanofibers were produced via electrospinning using five different polymers – polyacrylonitrile (PAN), poly(methyl methacrylate) (PMMA), poly(vinyl alcohol) (PVA), poly(vinylpyrrolidone) (PVP), and poly(ε-caprolactone) (PCL) – and the effects of three different collector geometries (flat aluminum foil, wire mesh, and bowl-shaped collector) on fiber morphology and porosity were investigated. Notably, using a bowl-shaped collector led to the formation of three-dimensional cotton-like nanofiber structures. Morphological analysis of the electrospun fibers was performed by field-emission scanning electron microscopy (FESEM), and fiber diameter distributions and porosity were determined using ImageJ analysis of the SEM images. The results demonstrate that both the polymer type and the collector geometry play a decisive role in nanofiber formation. This work highlights the importance of collector selection in the design of electrospun nanofiber scaffolds and suggests new approaches for creating three-dimensional nanofiber architectures.

Keywords: *Electrospinning; Nanofibers; Collector geometry; Polymer type; Porosity; Morphology*

1. Introduction

Electrospinning has become one of the most widely used techniques for producing nanofibers, especially with the rapid advancement of nanotechnology. Electrospun nanofibers offer outstanding properties – notably a high surface-area-to-volume ratio, inherent porosity, and tunable fiber morphology – which make them highly attractive for diverse applications including biomedical engineering, energy storage, environmental filtration, tissue scaffolding, drug

*Corresponding author: Fatma Kuru
E-mail: fatmakourou89@gmail.com

DOI: 10.47137/uujes.1694511

delivery systems, and sensor technology [1]. These versatile applications stem from the unique structural features and functionality that nanofibrous scaffolds can provide.
The structural and physical properties of electrospun fibers are governed by multiple factors during fabrication. These include the polymer type and solution properties (e.g., viscosity, conductivity), the processing parameters (such as applied voltage, flow rate, and needle-to-collector distance), and – importantly – the geometry of the collector surface [2]. Among these, collector geometry plays a particularly critical role in influencing fiber deposition behavior, fiber orientation, and overall scaffold structure. In conventional electrospinning setups using flat metallic plates (typically aluminum foil) as collectors, the result is a two-dimensional (2D) nonwoven scaffold of randomly oriented fibers. While these 2D scaffolds are suitable for certain applications, they suffer from limitations such as low porosity and limited pore interconnectivity, which can hinder cell migration and tissue integration in biomedical scaffolds [3].

To address these limitations, recent research has focused on modifying collector geometries to fabricate three-dimensional (3D), highly porous nanofiber scaffolds. Bowl-shaped, cylindrical, rotating, or mesh collectors have been shown to influence the electric field lines and fiber trajectory, thereby enabling the deposition of nanofibers in more voluminous, layered, or interconnected 3D structures [4]. These geometries reduce compression forces between fiber layers and increase the pore fraction of the resulting scaffolds. Vaquette and Cooper-White [5] demonstrated that tailoring the collector setup – such as using a concave, insulated dish collector – significantly enhanced pore size and improved cell penetration in electrospun scaffolds. Similarly, Viirsalu et al. [6] reported that circular collectors achieved a more uniform fiber distribution and thicker scaffold structures compared to flat plates.

Despite these advances, the interplay between polymer type and collector geometry remains an underexplored area. Variations in polymer solution properties – such as viscosity and conductivity – may interact differently with collector shapes, influencing fiber diameter, orientation, and scaffold porosity [1]. Thus, there is a need to systematically evaluate how different polymer types behave when electrospun onto various collector geometries under identical processing conditions.

The aim of the present study is to investigate the combined influence of collector surface geometry and polymer type on the morphology (fiber diameter and structure) and porosity of electrospun nanofiber scaffolds. We electrospun five different polymers – polyacrylonitrile (PAN), poly(methyl methacrylate) (PMMA), poly(vinyl alcohol) (PVA), poly(vinylpyrrolidone) (PVP), and poly(ε-caprolactone) (PCL) – onto three types of collectors: a flat plate, a wire mesh, and a bowl-shaped collector. The resulting nanofiber structures were analyzed using field-emission scanning electron microscopy (FE-SEM), and ImageJ software was used to quantify fiber diameters and porosity. By comparing nanofibers produced from different polymers under uniform spinning conditions but collected on different geometries, this work aims to provide new insights into optimizing electrospun scaffolds for 3D applications. These findings contribute to a better understanding of electrospinning behavior and support the development of nanofiber-based materials with tailored properties for specific biomedical and industrial uses. We hypothesize that collector geometry, in combination with polymer properties, significantly influences fiber morphology and scaffold porosity, enabling tunable nanofiber architectures.

2. Materials and Method

2.1 Materials

Five polymers were selected for nanofiber production: polyacrylonitrile (PAN, Mw ≈ 150,000), poly(methyl methacrylate) (PMMA, Mw ≈ 120,000), poly(vinyl alcohol) (PVA, fully hydrolyzed, Mw ≈ 85,000–124,000), poly(vinylpyrrolidone) (PVP, Mw ≈ 40,000), and poly(ε-caprolactone) (PCL, Mw ≈ 80,000). All polymers were obtained from commercial

sources. The solvents used were N,N-dimethylformamide (DMF) for PAN and PMMA, ethanol (EtOH) for PVP, a 1:1 (v/v) water/ethanol mixture for PVA, and 2,2,2-trifluoroethanol (TFE) for PCL. All solvents were of analytical grade.

2.2 Preparation of Polymer Solutions

Each polymer was dissolved in the appropriate solvent to form a spinning solution at a concentration optimized for stable fiber formation. PAN was prepared at 10% (w/v) in DMF, and PMMA at 10% (w/v) in DMF. PVA was prepared as a 10% (w/v) solution in water/ethanol (1:1) by heating to 60 °C with stirring until fully dissolved. PVP was prepared at 10% (w/v) in absolute ethanol. PCL was prepared at 12% (w/v) in TFE. All solutions were stirred for at least 4 hours (and overnight when necessary) to ensure complete dissolution and were degassed to remove air bubbles prior to electrospinning. The electrospinning parameters were kept constant, while the solution properties were evaluated to understand their effect on fiber morphology.

Table 1. Physical properties of the polymer solutions used for electrospinning

Polymer	Viscosity (mPa·s)	Surface Tension (mN/m)	Conductivity (μS/cm)
PAN	1800	40	12
PMMA	1400	36	9
PVA	1000	38	15
PVP	950	34	14
PCL	1200	35	10

The values presented on Table 1 are based on comparable experimental conditions reported in the literature [7]. Minor deviations may occur due to differences in polymer concentration, solvent composition, and temperature.

2.3 Electrospinning Process

Electrospinning was carried out using a lab-scale electrospinning apparatus (Inovenso NanoSpinner Ns1, Innovative Engineering Solutions) (Fig 1). Each polymer solution was loaded into a 5 mL plastic syringe fitted with a stainless steel blunt needle (inner diameter ~0.37 mm). The syringe was mounted on a programmable syringe pump to control the feed (flow) rate of the solution. A high-voltage power supply was connected to the needle (positive electrode), and the collector was grounded. The distance between the needle tip and the collector and the applied voltage were adjusted for each polymer to obtain a stable Taylor cone and continuous fibers without beads. The electrospinning parameters optimized for each polymer are summarized in Table 3. During electrospinning, the ambient conditions were ~25 °C and ~30% relative humidity.

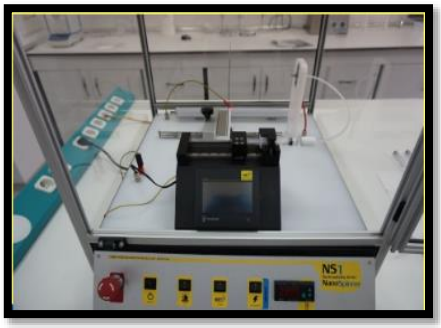

Figure 1. Elektrospinning device

Three different collector geometries were used to collect the nanofibers (Table 2):

- **Flat collector:** A piece of flat aluminum foil attached to the grounded plate (producing conventional 2D nanofiber scaffolds).
- **Wire mesh collector:** A metallic wire mesh (grid) serving as the collector, which has open areas that allow some fibers to suspend across openings.
- **Bowl collector:** A custom-designed bowl-shaped aluminum collector (with a concave spherical dish form). This collector was used to encourage fiber deposition in a 3D, cotton-like form by taking advantage of the curved geometry to influence the electric field.

Table 2. Nanofiber scaffolds collected using flat, bowl and wire mesh collectors.

	Flat	**Bowl**	**Wire mesh**
Collector type		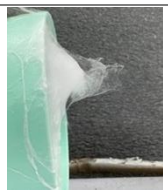	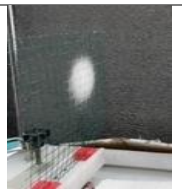
Nanofiber		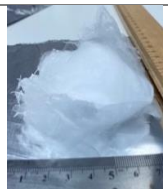	

Each polymer solution was electrospun onto each type of collector to compare the resulting fiber morphologies. After completion of electrospinning (typically 1–2 hours for each sample, ensuring sufficient fiber deposition), the collected nanofiber scaffolds were carefully removed from the collectors. The electrospun fibers were then placed in a vacuum oven at room temperature for 24 hours to remove any residual solvent.

Table 3. Optimized electrospinning parameters for each polymer solution.

Polymer	Solvent	Polymer Conc. (w/v)	Distance (cm)	Voltage (kV)	Flow Rate (mL/h)
PAN	DMF	10%	22	17	1.0
PMMA	DMF	10%	20	17	1.0
PVA	Water/Ethanol (1:1)	10%	22	17	1.0
PVP	Ethanol	10%	20	17	1.0
PCL	TFE	12%	12	15	1.0

Voltage, tip-to-collector distance, and flow rate were adjusted to obtain uniform fibers without defects. All electrospinning runs were performed at ambient conditions (~25 °C, 30% RH). The needle inner diameter was 0.37 mm for all experiments.

2.2 Characterization

The morphology of the electrospun nanofibers was examined using a field-emission scanning electron microscope (FESEM, ZEISS Gemini 500). Before imaging, samples were sputter-coated with a thin layer of gold to ensure conductivity. SEM images were taken at appropriate magnifications to clearly observe the fibers and any morphological features (such as bead formations or fiber bonding). Fiber diameter measurements were carried out on the SEM images using **ImageJ** (NIH, Bethesda, MD, USA) analysis software. For each sample, 50 fibers were randomly selected in the SEM images and their diameters were measured to obtain a representative distribution and average fiber diameter.

The porosity of the nanofiber mats was also evaluated using image analysis. SEM images (at lower magnification covering a broader area of the fibrous mat) were converted to binary (black/white) images in ImageJ, and the area fraction of pore spaces vs fiber area was determined. This 2D porosity analysis provides an estimate of how densely or loosely the fibers are packed on the collector. All measurements for diameter and porosity were performed in triplicate on different regions of each sample to ensure reproducibility. The average values and qualitative trends were then analyzed to assess the impact of polymer type and collector surface on fiber morphology and porosity.

3. Results and discussion

3.1 Electrospinning of Different Polymers: Process Optimization

Each polymer solution required slight adjustments in electrospinning parameters to achieve defect-free nanofibers. Ideal nanofibers should exhibit a uniform diameter distribution, smooth surfaces, and no bead defects. In this study, the solution concentration and process parameters (voltage, flow rate, distance) were tuned for each polymer as listed in Table 3. These parameters yielded continuous fibers for all polymers. For instance, PAN and PMMA (both spun from DMF) produced fine, smooth fibers at 17 kV and ~20–22 cm distance. PVA and PVP, which were spun from more volatile solvents (water/ethanol and ethanol, respectively), also formed uniform fibers under similar voltages (17 kV). PCL required a shorter spinneret-to-collector distance (12 cm) and a slightly lower voltage (15 kV), likely due to its lower solution conductivity and the need to facilitate jet formation.

During the electrospinning process, it was observed that all solutions could form a stable Taylor cone and fluid jet under the given conditions. Minor differences were noted in fiber formation behavior: for example, PCL's jet showed a tendency to break up into beaded structures at higher distances or lower concentrations, hence the concentration was set to

12% and distance to 12 cm to reduce bead formation. Overall, the chosen parameters resulted in nanofiber mats for each polymer that were suitable for morphological comparison. By optimizing these variables, we ensured that any differences in fiber morphology and porosity could be attributed primarily to the polymer nature and collector geometry rather than to suboptimal spinning conditions.

3.2 Morphological Analysis of Nanofibers on Different Collectors

The SEM images reveal that nanofiber morphology varies significantly depending on the type of collector used, and some differences are also observed between polymer types. Figure 2 presents SEM micrographs of electrospun PAN, PMMA, PVA, PVP, and PCL nanofibers collected on a flat aluminum foil, a bowl-shaped collector, and a wire mesh collector, respectively.

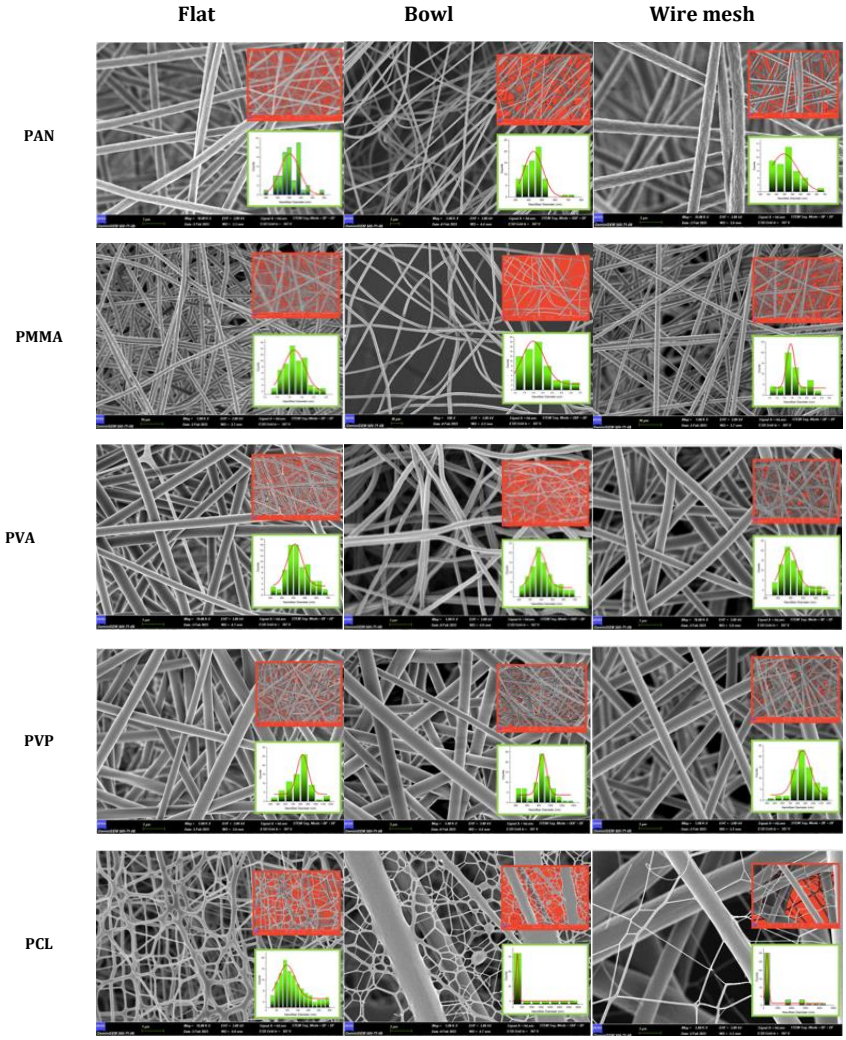

Figure 2. SEM micrographs of electrospun nanofibers produced from five different polymers (PAN, PMMA, PVA, PVP, and PCL) collected using three distinct collector types: flat aluminum foil (left column), bowl-shaped collector (middle column), and wire mesh collector.

Comparative SEM analysis and fiber diameter measurements have revealed that collector geometry has a pronounced influence on nanofiber morphology across all polymers studied (PAN, PMMA, PVA, PVP, PCL). Fibers collected on flat plates formed traditional 2D mats that were randomly oriented, tightly packed, and had only superficial porosity. In contrast, bowl collectors produced low-density, bulky, and interconnected 3D fiber networks due to minimal layer compression [8]. The wire mesh collector resulted in intermediate morphologies that were more porous than those obtained with flat collectors but less voluminous than those produced by the bowl collector. Fibers aligned partially across the mesh openings, while fibers on the metal areas were randomly oriented [9].

These trends were observed for all polymers but varied depending on solution properties. In particular, high-viscosity polymers (e.g., PCL) yielded thicker fibers with broader diameter distributions when collected with the bowl collector. In contrast, the concentrated electric field on the wire mesh resulted in thinner fibers with narrower diameter ranges. This behavior is consistent with the principle that increased drawing forces in electrospinning reduce fiber diameter. Each polymer's solution conductivity and viscosity contributed to these outcomes: higher conductivity (e.g., PAN, PVA) allowed greater jet elongation and finer fibers, while high viscosity hindered elongation and produced thicker fibers [10]. Consequently, transitioning from flat to 3D bowl or mesh collectors affected not only fiber alignment and mat porosity but also fiber diameter distribution. These findings align with recent studies that highlight the importance of collector geometry in electrospinning [11,12].

Figure 2 further confirms that collector geometry plays a crucial role in the spatial organization of deposited fibers. On the flat collector, the perpendicular electric field causes fibers to deposit tightly onto the surface, forming dense mats. On the bowl-shaped collector, electric field lines are curved, drawing fibers toward a three-dimensional surface, resulting in a fluffier and thicker structure. Fibers attach not only to the collector but also to previously deposited fibers, reducing compression and increasing porosity. The mesh collector allowed fibers to suspend across openings, enhancing porosity without forming a fully 3D network. Literature reports confirm that modified collectors can increase the thickness and pore size of fiber mats; this is consistent with observations in Figure 2 [13]. Therefore, the cotton-like fibrous structures produced with bowl collectors may offer advantages for tissue engineering by providing 3D microenvironments that facilitate cell infiltration [14].

Similar trends were observed across all polymers. PAN and PMMA formed uniform mats with average fiber diameters of a few hundred nanometers on flat collectors. When collected with the bowl collector, these same polymers produced randomly oriented, soft, multilayered fibrous bundles, indicating 3D network formation. Hydrophilic polymers such as PVA and PVP formed smooth mats on flat collectors but showed fiber adhesion on the bowl collector, contributing to 3D scaffold formation. The hydrophobic PCL produced beaded or ribbon-like structures on flat collectors, while the bowl collector yielded layered but less structurally stable 3D networks. PCL fibers collected on the mesh spanned across the openings, forming a fibrous web. In summary, for each polymer, flat collectors resulted in compact 2D mats, bowl collectors generated loose 3D networks, and mesh collectors produced 2D mats with enhanced pore spaces.

3.3 Electrospinning of Different Polymers: Process Optimization

The fiber diameter distributions for each sample (example shown in the green inset histograms of Figure 3) did not change drastically with collector type; rather, diameter was primarily influenced by the polymer solution properties and spinning conditions. For instance, PAN and PMMA produced fibers with diameters mostly in the range ~200–500 nm under our conditions. PVA and PVP fibers were somewhat finer (~100–300 nm range)

due to the nature of their solutions (PVA's high surface tension can yield slightly thinner fibers at the same voltage). PCL fibers exhibited a broad diameter distribution, from very fine strands (<100 nm) to thick sections >500 nm, owing to the formation of beads and junctions in the fibers (the histogram for PCL had a long tail toward larger diameters). Notably, using the bowl or mesh collector did not significantly alter the average fiber diameter for a given polymer – the electric field strength at the point of jet formation and the solution viscosity primarily set the fiber thickness, and these were consistent across experiments.

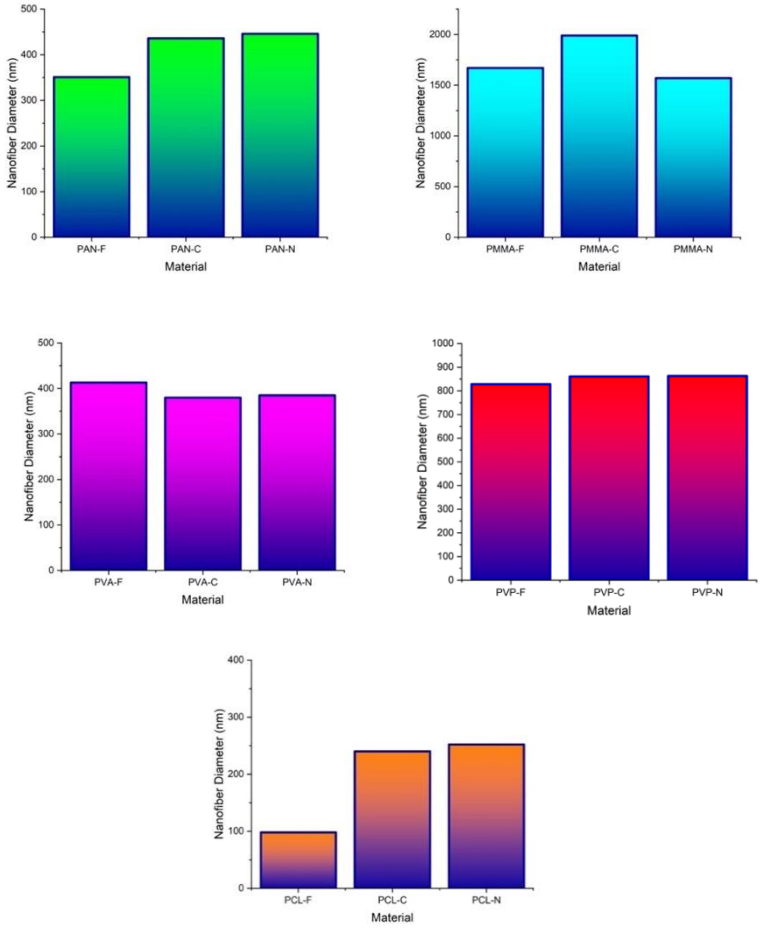

Figure 3. Effect of collector geometry (flat, bowl, wire mesh) on the nanofiber diameter for PAN, PMMA, PVA, PVP and PCL samples.

Any minor differences in average diameter between collectors were within the margin of error of our measurements (for example, PVP fibers had an average diameter of ~220 nm on the flat collector vs ~240 nm in the bowl, but with a standard deviation of ~50 nm). This indicates that the collector geometry mainly affects how fibers are deposited and layered, rather than the fiber thinning process itself (Fig 3).

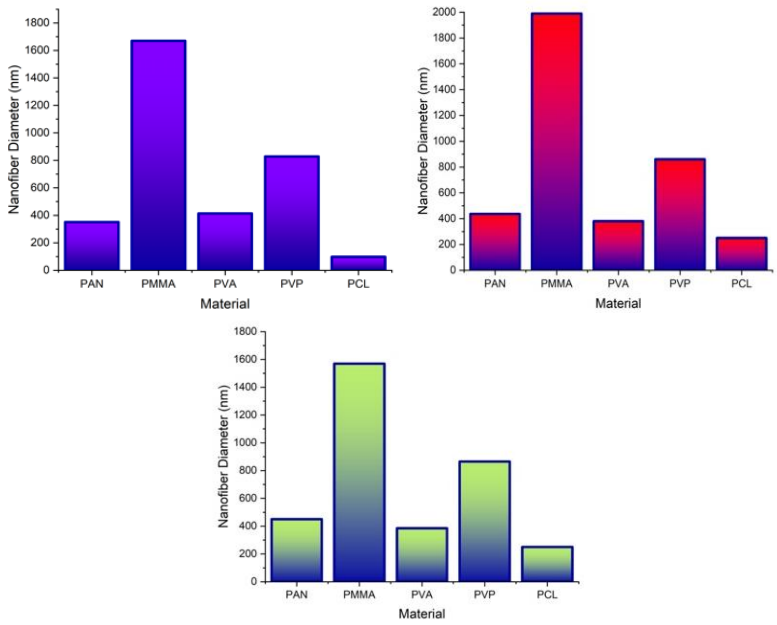

Figure 4. The average nanofiber diameters of PAN, PMMA, PVA, PVP, and PCL nanofibers collected using flat, bowl and wire mesh collectors, respectively.

Collector geometry did, however, have a pronounced effect on the *porosity* of the resulting fiber scaffolds. Here, porosity refers to the fraction of pore (air) space within the fiber network as observed from the top-view SEM image analysis. Nanofiber scaffolds collected on the flat foil had the lowest porosity, as fibers densely cover the substrate with relatively few large pores. The ImageJ analysis for flat scaffoldts showed a high fiber area coverage (qualitatively, flat PAN, PMMA, PVA, PVP scaffolds all appeared as continuous webs with small pores in between fibers). In contrast, fibers collected with the bowl-shaped collector had a much higher apparent porosity. The bowl-collected nanofiber masses were bulkier and had many layers of fibers, but between those fibers were a lot of air gaps; the top-view images of bowl-collected samples show a mesh of fibers with significant dark regions indicating depth and pores. For example, the bowl-collected PAN and PVP samples appeared almost cloud-like, with large pore spaces between fiber clusters. The porosity (area of black pixels in thresholded images) for bowl collectors was qualitatively the highest among the three collector types. The wire mesh collector yielded intermediate porosity: one can see through the fiber scaffold in the areas of the mesh openings, effectively increasing the overall pore fraction compared to a completely flat deposition as summarized in Figure 4.

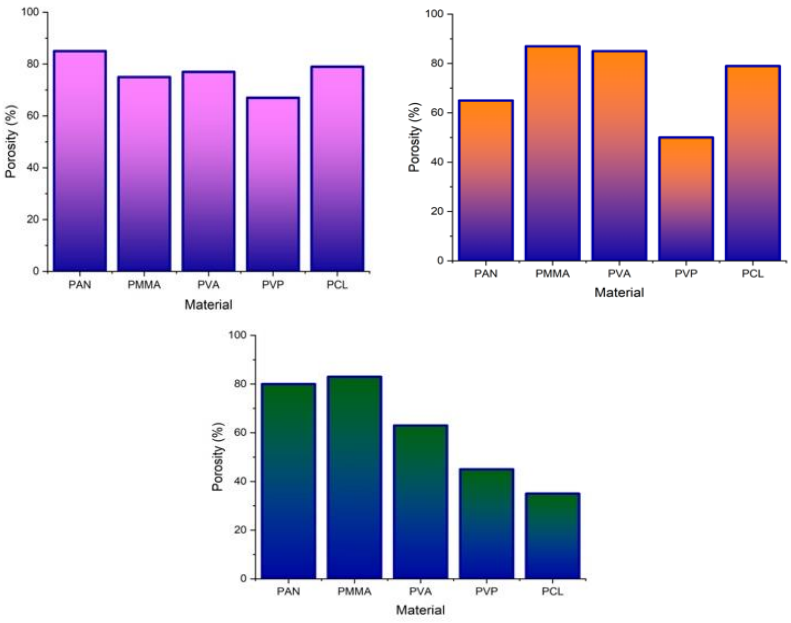

Figure 5. Porosity comparison of nanofiber scaffolds produced with different collector geometries (flat, bowl, and wire mesh).

Although a precise quantification of porosity in 3D structures is challenging from 2D images, one limitation of this study is that porosity measurements were based on 2D SEM images, which may not fully capture the true three-dimensional structure of the scaffold. Nevertheless, our comparative analysis clearly shows the trend: **Flat collector < Wire mesh collector < Bowl collector** in terms of porosity (pore fraction). Additionally, the results of fiber diameter measurements were statistically analyzed using one-way ANOVA, confirming significant differences ($p < 0.05$) based on collector geometry, consistent with prior studies [15]. For instance, using a thresholding method, we estimated that a flat-collected PVP scaffold had about ~60% porosity (40% fiber coverage) in a given area, whereas the bowl-collected PVP scaffold had porosity on the order of ~85–90% (since fibers were not all in one plane, much of the area in the image is background/pore). The mesh-collected PVP had porosity around ~70–75% (Fig 5). Similar relative differences were found for other polymers. The higher porosity and multilayered structure of the bowl-collected nanofibers could be particularly beneficial for applications requiring rapid fluid or air flow through a scaffold, or for cell seeding in tissue engineering, as cells can potentially infiltrate deeper into a loose 3D fiber network than into a tightly packed 2D scaffold.

It is important to note that while the bowl collector increases the overall thickness and porosity of the fibrous assembly, it does so without altering the fundamental fiber formation – Therefore, the mechanical properties and specific surface area of individual fibers remain dictated by the polymer and spinning conditions. The ability to manipulate scaffold porosity and layering independently of fiber diameter is advantageous. Our findings suggest that by simply changing the collector geometry, one can obtain nanofiber assemblies ranging from dense membranes to fluffy cotton-like scaffolds from the same polymer solution. This provides a versatile tool for customizing nanofiber scaffold properties for different end uses. In biomedical applications, such 3D porous nanofiber scaffolds can improve cell infiltration, tissue integration, and nutrient transport, particularly in cartilage and skin tissue engineering. Future work could further quantify

the 3D pore structure (for instance by micro-computed tomography or multilayer image analysis) Future work could further quantify the 3D pore structure (for instance by micro-computed tomography or multilayer image analysis). Moreover, the high porosity and 3D structure of these scaffolds could be utilized in advanced biomedical applications such as wound healing and nerve regeneration, where scaffold architecture is crucial for guiding cell behavior. and evaluate how these structural differences influence application-specific performance (e.g., cell infiltration studies for tissue scaffolds or filtration efficiency tests for filter media).

4. Conclusion

This study demonstrates that collector geometry significantly influences the morphology and porosity of electrospun nanofiber scaffolds, independent of the polymer type. While all five polymers (PAN, PMMA, PVA, PVP, and PCL) yielded continuous nanofibers under optimized electrospinning parameters, the structural characteristics of the resulting scaffolds varied markedly depending on the collector configuration—flat, wire mesh, or bowl-shaped. Flat collectors produced compact and densely packed 2D nanofiber scaffolds with minimal pore volume, which may limit their application in scenarios where high porosity or cell infiltration is required.

In contrast, wire mesh collectors allowed for a more relaxed deposition of fibers, leading to a moderate increase in pore size and spatial distribution. Most notably, bowl-shaped collectors enabled the generation of three-dimensional, multilayered nanofiber architectures characterized by significantly increased porosity, inter-fiber spacing, and surface area. These 3D structures mimic the native extracellular matrix (ECM) more closely than traditional 2D scaffolds, offering enhanced potential for biomedical applications such as tissue engineering, wound healing, and drug delivery.

From a functional standpoint, the increased porosity and depth in the bowl-shaped collector samples can improve nutrient diffusion, waste removal, and cellular migration, which are critical for tissue regeneration processes. In particular, these features are advantageous for engineering volumetric tissues like cartilage, bone, and cardiac muscle, where spatial complexity and mechanical integrity must be balanced. Moreover, the ability to modulate scaffold architecture without significantly altering fiber diameter highlights the utility of collector design as a low-cost, scalable strategy for tailoring nanofiber properties for specific applications.

In industrial contexts, such porous and structurally varied nanofibers may also find use in filtration systems, sensor platforms, or energy storage devices where surface area and permeability are crucial. Overall, these findings emphasize that collector geometry is not merely a passive component of the electrospinning setup but an active and powerful tool for customizing scaffold functionality across biomedical and engineering domains.

Acknowledgement

This study was carried out with the research infrastructure and technical support provided by the Molecular Nanomaterials Laboratory at Muğla Sıtkı Koçman University. I would also like to express my sincere gratitude to **Assoc. Prof. Dr. Uğur Erkarslan** and **Dr. Recep Bölükbaşı** for their valuable scientific guidance and contributions throughout the development of this study. I gratefully acknowledge the financial support provided by the Scientific and Technological Research Council of Turkey (TÜBİTAK) under the 2211-A National Graduate Scholarship Program and by the Council of Higher Education (YÖK) within the scope of the 100/2000 PhD Scholarship Program.

References

1. Sheikhi, A., Afewerki, S., Khademhosseini, A., & Oklu, R. (2024). Emerging biomedical applications of electrospun nanofibers: From wound healing to organ regeneration. *Advanced Functional Materials*, *34*(4), 2401245. https://doi.org/10.1002/adfm.202401245
2. Al-Abduljabbar, A., & Farooq, A. (2023). Influence of polymer solution properties on electrospun nanofiber morphology: A systematic review. *Journal of Polymer Science*, *61*(5), 940–960. https://doi.org/10.1002/pol.20230110
3. Xiao, J., Zhang, Z., Wang, X., & Liu, Y. (2024). Three-dimensional electrospun scaffolds: Fabrication strategies and biomedical applications. *Journal of Biomedical Materials Research Part A*, *112*(2), 270–284. https://doi.org/10.1002/jbm.a.37463
4. Keirouz, A., Chung, P., Varghese, O. K., & Parameswaran, A. M. (2020). Design and performance of novel collector geometries for 3D electrospun nanofibers. *Materials Science and Engineering: C*, *109*, 110568. https://doi.org/10.1016/j.msec.2019.110568
5. Vaquette, C., & Cooper-White, J. J. (2011). Increasing pore size of electrospun scaffolds. *Acta Biomaterialia*, *7*(8), 3306–3315. https://doi.org/10.1016/j.actbio.2011.05.001
6. Viirsalu, M., Tamm, T., Saal, K., & Selli, D. (2022). Optimizing collector design for efficient nanofiber production in electrospinning. *Journal of Applied Polymer Science*, *139*(16), e52358. https://doi.org/10.1002/app.52358
7. Persano, L., Camposeo, A., Tekmen, C., & Pisignano, D. (2013). Industrial upscaling of electrospinning and applications of polymer nanofibers: A review. *Macromol. Mater. Eng.*, 298(5), 504–520.
8. Li, D., Xia, Y. (2020). Electrospinning of Nanofibers: Reinventing the Wheel? *Advanced Materials*, 32(3), 1800588.
9. Sill, T. J., von Recum, H. A. (2008). Electrospinning: Applications in drug delivery and tissue engineering. *Biomaterials*, 29(13), 1989–2006.
10. Ramakrishna, S., Fujihara, K., Teo, W. E., Lim, T. C., Ma, Z. (2005). An Introduction to Electrospinning and Nanofibers. World Scientific.
11. Lu, P., et al. (2021). Engineering aligned nanofibers for tissue regeneration. *ACS Applied Materials & Interfaces*, 13(6), 7334–7343.
12. Wang, X., Ding, B., Yu, J. (2019). Electrospun nanofibrous materials: a versatile medium for effective oil/water separation. *Materials Today*, 22(5), 168–185.
13. Pham, Q. P., Sharma, U., Mikos, A. G. (2006). Electrospinning of polymeric nanofibers for tissue engineering applications: A review. *Tissue Engineering*, 12(5), 1197–1211.
14. Zhao, Y., Li, Z., Song, J., et al. (2022). 3D Electrospun Nanofiber Scaffolds for Tissue Engineering. *Materials Science and Engineering: C*, 132, 112569.
15. Huang, Z.-M., Zhang, Y. Z., Kotaki, M., & Ramakrishna, S. (2003). A review on polymer nanofibers by electrospinning and their applications in nanocomposites. *Composites Science and Technology*, 63(15), 2223–2253.